The charge dependence of cosmic-ray modulation in a Fisk-type heliospheric magnetic field

SHOKO MIYAKE[1], SHOHEI YANAGITA[2]
[1]*College of Community Development, Tokiwa University, Mito, Ibaraki 310-8585, Japan*
[2]*Faculty of Science, Ibaraki University, Mito, Ibaraki 310-8512, Japan*
miyakesk@tokiwa.ac.jp
DOI: 10.7529/ICRC2011/V11/0971

Abstract: The differences between the effect of a Parker heliospheric magnetic field (HMF) and a Fisk-type HMF on the charge dependence of cosmic-ray modulation have been investigated. We have developed fully time-dependent and three-dimensional codes for cosmic-ray modulation in a Fisk-type HMF. The calculation of the propagation of galactic cosmic ray in the heliosphere is made by solving a coupled set of stochastic differential equations (SDE) which is equivalent to the Parker's convection-diffusion equation. Our numerical results show that the latitudinal dependence of cosmic-ray intensities in the Fisk-type HMF is greatly different from the dependence in the Parker HMF, especially at the heliospheric polar region. We have also confirmed that the sample trajectories of cosmic ray in the Fisk-type HMF show clear tendencies to deviate from the typical drift pattern in the Parker HMF. These results are, in principle, consistent with some results observed by Ulysses spacecraft at high latitudes.

Keywords: galactic cosmic ray, charge dependence of modulation, heliopheric magnetic field

1 Introduction

The heliospheric magnetic field (HMF) plays most important role in the model for the solar modulation. A standard Parker HMF [1] has been successfully used in modulation studies, however, this model may be an oversimplification to describe the field in the polar region of the heliosphere. The model for HMF by Fisk (1996) [2] which takes account of the interplay between the differential rotation of the photosphere of the Sun, and the nonradial expansion of the solar wind in the solar corona. This model suggests large excursions of the HMF in latitude. This model may potentially be able to account for the observations from the Ulysses spacecraft of recurrent energetic particle event at high latitudes (Simpson et al. [3]; Zhang [4]; Paizis et al. [5]) and the smaller-than-expected cosmic-ray intensities observed at high latitudes [6].

We have developed a fully time-dependent and three-dimensional code to study the galactic cosmic-ray modulation in a Fisk-type HMF. The calculation of the propagation of galactic cosmic ray in the heliophere is made by solving a coupled set of stochastic differential equations (SDE) which is equivalent to the Parker's convection-diffusion equation. The stochastic numerical codes adapted for the wavy heliospheric current sheet in a Parker HMF has been developed by Miyake and Yanagita [7]. We have developed this stochastic code into the code for the Fisk-type HMF. In this paper we present the differences between the effect of the Parker HMF and the Fisk-type HMF on the charge dependence of galactic cosmic-ray modulation.

2 Numerical Model

Transport of the galactic cosmic rays in the heliosphere is described by the Parker's convection-diffusion equation. This convection-diffusion equation is equivalent to a coupled set of the SDE [8, 9]. The SDE equivalent to the diffusion convection partial differential equation is written as

$$\begin{aligned} d\mathbf{X} &= (\boldsymbol{\nabla}\cdot\boldsymbol{\kappa} - \mathbf{V_{sw}} - \mathbf{V_d})\,dt + \textstyle\sum_s \boldsymbol{\sigma}_s dW_s(t)\,, \\ dP &= \tfrac{1}{3}P\,(\boldsymbol{\nabla}\cdot\mathbf{V_{sw}})\,dt\,, \end{aligned} \tag{1}$$

where $\mathbf{X}$ and P are the guiding center and the momentum of the galactic cosmic-ray particle, $\mathbf{V_{sw}}$ is the solar wind velocity, $\mathbf{V_d}$ is the gradient-curvature drift velocity, $\boldsymbol{\kappa}$ is the diffusion coefficient tensor, $\sum_s \sigma_s^\mu \sigma_s^\nu = 2\kappa^{\mu\nu}$, and dW_s is a Wiener process given by the Gaussian distribution. We adopted $V_{sw} = 800\mathrm{km/s}$, $\kappa_\parallel = 1.5 \times 10^{21}\beta(p/(1GeV/c))(Be/B)\ \mathrm{cm^2/s}$ and $\kappa_\perp = 0.05\kappa_\parallel$. We have used the "drift velocity field method" [10] for the calculation of drift in the heliospheric current sheet.

In our simulation, particles start at 1 AU on the equatorial plane and run backward in time until they exit the heliospheric boundary, 90 AU. The momentum spectrum $f_{\mathbf{X}}(p)$ at arbitrary position $\mathbf{X}$ is written as a convolution of the spectrum $f_{\mathbf{X_0}}(p_0)$ at the heliospheric boundary with the normalized transition probability $F(p_0, \mathbf{X_0}|p, \mathbf{X})$ obtained by our SDE method as

$$f_{\mathbf{X}}(p) = \int f_{\mathbf{X_0}}(p_0) F(p_0, \mathbf{X_0}|p, \mathbf{X}) dp_0\,. \tag{2}$$

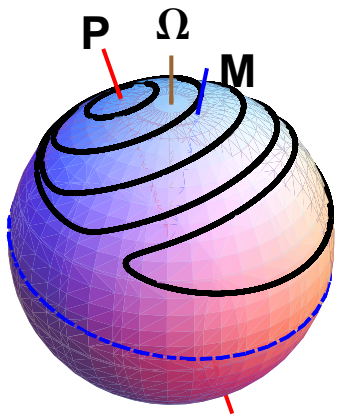

Figure 1: The trajectories of the footpoints of the magnetic field lines on the source surface in the frame corotating with the Sun (solid curve) and resultant differential rotational axis (P-axis). The Ω-axis indicates the rotational axis. The M-axis indicates the magnetic axis of the HMF.

Burger and Hitge (2004) [11] described a divergence-free Fisk-Parker hybrid HMF that should be a reasonable approximation for the case when field lines open into the heliosphere both in the polar coronal holes and at low latitudes. This HMF model reproduces the trajectories of the footpoints of the magnetic field lines on the source surface which are similar to the trajectories discussed by Fisk et al. (1999) [12], however, it is different from the model by Fisk et al. (1999) in the azimuthal direction of the trajectories.

In this paper, we have developed the Burger's divergence-free Fisk-Parker hybrid HMF to the Fisk-type HMF. In the frame corotating with the Sun, the meridional and azimuthal components of the velocity of a footpoint of the magnetic field lines on the source surface are given by

$$\begin{aligned} u_\theta|_\Omega = \; & -r\omega \sin\phi \, [\, Fs(\delta) \sin\beta \\ & - \sin\alpha \sin(\alpha+\beta) \; \times \; (\cos\theta \sin\alpha \\ & - \cos\alpha \cos\phi \sin\theta \,) \, \frac{\mathrm{d}\, Fs(\delta)}{\mathrm{d}\,\delta} \, , \\ u_\phi|_\Omega = \; & -r\omega \, [\, Fs(\delta) \, (\cos\theta \cos\phi \sin\beta \\ & + \cos\beta \sin\theta) - \sin(\alpha+\beta) \\ & \times (\cos\theta \cos\phi \sin\alpha \; - \; \cos\alpha \sin\theta) \\ & \times (\cos\theta \sin\alpha \; - \; \cos\alpha \cos\phi \sin\theta) \\ & \frac{\mathrm{d}\, Fs(\delta)}{\mathrm{d}\,\delta}] \, . \end{aligned} \tag{3}$$

Here $\delta = \cos(\alpha)\cos(\theta) + \cos(\phi)\sin(\alpha)\sin(\theta)$. ω is the differential rotation rate. We assume $\omega = \Omega/4$, where Ω is the equatorial rotation rate of the Sun.

The angle β is the angle between the rotational axis (Ω-axis) and the differential rotational axis (P-axis) on the source surface as shown in figure 1. The angle β is related to three angles : (1) the tilt angle α of the heliospheric current sheet; (2) the polar angle θ_{CH} of the coronal hole boundaries in the heliomagnetic coordinates on the photosphere; (3) the polar angle Θ_{CH} of the coronal hole boundaries on the source surface,

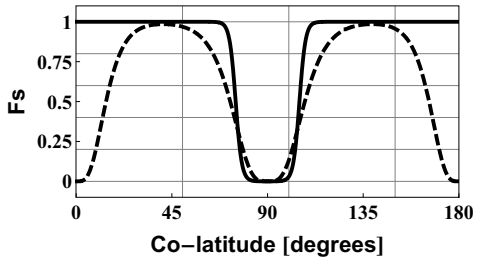

Figure 2: The transition function Fs used in this study (solid line) and used in Burger and Hitge [11] (dashed line).

$$\beta = \cos^{-1}\left[1 - (1-\cos\Theta_{CH})\,\frac{\sin^2\alpha}{\sin^2\theta_{CH}}\right] - \alpha \, . \tag{4}$$

We assume $\theta_{CH} = 24°$, $\Theta_{CH} = 75°$ and $\alpha = 10°$. We take this value for α as the average tilt angle during the time of BESS observation as shown later.

The transition function Fs controls the transition between the Parker field and the Fisk field. When $Fs = 1$, the HMF is reduced to the Fisk field, and when $Fs = 0$, the Parker field is attained. It is not clear whether differential rotation persists in the polar regions, however the results obtained by helioseismology (e.g., Schou et al. [13]) suggests that the differential rotation also occurs in the polar region of the Sun. In this paper we assume the differential rotation persists in the polar regions, and we adopt

$$Fs = \begin{cases} \dfrac{1}{1+\exp(-k1+k2)} & \text{(at north hemisphere)} \\ \dfrac{1}{1+\exp(k1-k2)} & \text{(at south hemisphere)} \end{cases} , \tag{5}$$

with

$$\begin{aligned} k1 &= 2\lambda\theta_M \, , \\ k2 &= 2\lambda\cos^{-1}(\delta) \, . \end{aligned} \tag{6}$$

Here $\lambda = 20$. Figure 2 shows the transition function Fs. The solid and dashed line indicates the Fs used in this study and Burger and Hitge (2004), respectively.

The Fisk-type HMF in the fixed heliocentric spherical polar coordinate (r, θ, ϕ) is represented as

$$B_r = A\left(\frac{1}{r^2}\right) \, , \tag{7}$$

$$\begin{aligned} B_\theta = \; & B_r \frac{r\omega}{V_{sw}} \sin\phi^* \, [\, Fs(\delta) \sin\beta \\ & - \sin\alpha \sin(\alpha+\beta) \; \times \; (\cos\theta \sin\alpha \\ & - \cos\alpha \cos\phi^* \sin\theta \,) \, \frac{\mathrm{d}\, Fs(\delta)}{\mathrm{d}\,\delta} \, , \end{aligned} \tag{8}$$

$$
\begin{aligned}
B_\phi = \quad & -B_r \frac{r\Omega \sin\theta}{V_{sw}} + B_r \frac{r\omega}{V_{sw}} \\
& \times [\, Fs(\delta)\, (\cos\theta \cos\phi^* \sin\beta \\
& + \cos\beta \sin\theta) \; - \; \sin(\alpha+\beta) \\
& \times (\cos\theta \cos\phi^* \sin\alpha \; - \; \cos\alpha \sin\theta) \\
& \times (\cos\theta \sin\alpha \; - \; \cos\alpha \cos\phi^* \sin\theta) \\
& \times \frac{\mathrm{d}\, Fs(\delta)}{\mathrm{d}\, \delta}] \,,
\end{aligned}
\tag{9}
$$

with

$$
\begin{aligned}
\delta \quad &= \cos\alpha \cos\theta \; + \; \cos\phi^* \sin\alpha \sin\theta \,, \\
\phi^* \quad &= \phi + \Omega\, t + \phi_0 + \frac{(r - R_{ss})\Omega}{V_{sw}} \,.
\end{aligned}
\tag{10}
$$

A is some constant characterizing the intensity of HMF including the polarity. R_{ss} is the radius of the source surface. t is the time. ϕ_0 is a constant.

We do not consider the effect of random motion of footpoints of the HMF discussed by Giacalone (1999, 2001) [14, 15]. Note that the Fisk-type HMF does not take account of the random motion of the footpoints and the expansion of the field line in the solar corona along the azimuthal direction.

3 Results

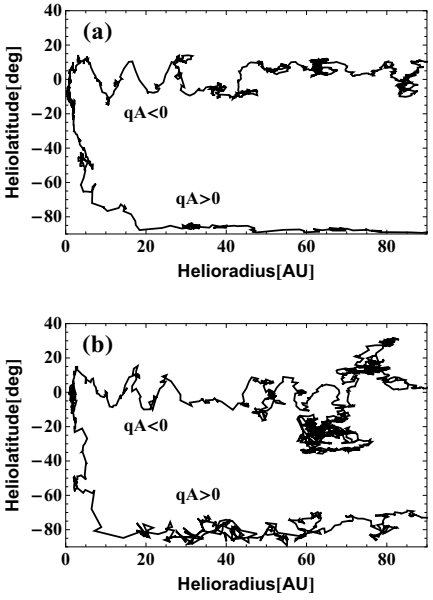

Figure 3: (a) Sample trajectory of protons with energy of 1 GeV at Earth in a Parker HMF.; (b) the same for a Fisk-type HMF.

Figure 3 shows sample trajectories of protons with energies of 1 GeV at the earth for the two types of HMF. In positive polarity $qA > 0$, protons drift in from the polar region to the equatorial plane while in negative polarity $qA < 0$, protons drift in along the wavy current sheet around the equatorial plane. This trend of the drift motions is common to the two types of HMF, however for the Fisk-type HMF protons tend to migrate to lower latitude region in $qA > 0$ while in $qA < 0$, protons show tendencies to move away from the current sheet when we compare to typical trajectories in the Parker HMF. These tendencies for a Fisk-type HMF are expected from disturbances in magnetic field lines caused by the differential rotation of the Sun.

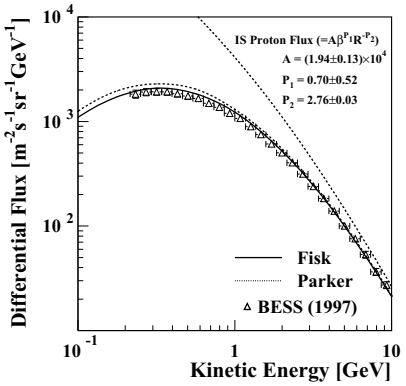

Figure 4: Simulated energy spectra for protons at Earth and observed proton energy spectrum in 1997.

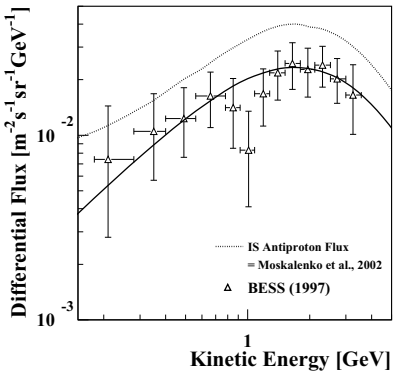

Figure 5: Simulated energy spectra for antiprotons at Earth and observed antiproton energy spectrum in 1997.

Energy spectra for the galactic cosmic-ray protons and antiprotons at Earth are shown in figure 4 and 5, respectively. The spectra obtained in our simulation for the Parker HMF are denoted by dashed lines and by solid lines for the Fisk-type HMF. We assume the local interstellar spectrum (LIS) of the protons is the same as shown in figure 8 of Shikaze et al. (2007) [16]. The LIS of the antiprotons is adapted from figure 7 of Moskalenko et al. (2002) [17]. The open triangles represents the energy spectra observed by BESS experiment in 1997 [16, 18]. The simulated spectrum for protons in the Fisk-type HMF agrees better with BESS results than the spectrum in the Parker HMF. The modulation level is much higher for $qA > 0$ in the Fisk-type HMF as expected from the trend of drift motions shown in figure 3. The simulated spectrum for antiprotons in the Fisk-type HMF also agrees well with BESS results.

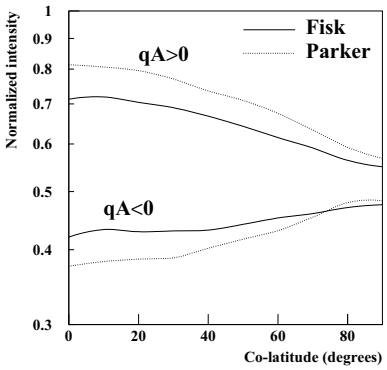

Figure 6: Latitudinal distribution of 1 GeV proton intensities at 1 AU.

The effects of the Fisk-type HMF on the cosmic-ray modulation are also demonstrated in the latitudinal dependence of the cosmic-ray intensities. Figure 6 shows 1 GeV proton intensities at 1 AU as a function of latitude. Dashed lines and solid lines indicate the cases for the Parker HMF and for the Fisk-type HMF respectively. For $qA > 0$, the intensity in the Fisk-type HMF is lower than the intensity in the Parker HMF. This trend originate from that protons which drift in from the polar region suffer from higher level modulation by the Fisk-type HMF at polar region. For $qA < 0$ the tendency of the intensities is opposite. This trend in intensities comes from the fact that protons which drift in along the current sheet have much higher chance to migrate into higher latitude region where particles can propagate faster. Figure 6 indicates also the difference in the intensities for the two types of HMF is much greater in the polar region than near the equatorial plane for both polarities of qA. This trend may also be understood by the reasons mentioned above. These effects seen in the Fisk-type HMF account for some observations which can't be accounted for in the Parker HMF such as the recurrent energetic particle event and the smaller-than expected GCR intensities at high latitudes observed by Ulysses spacecraft (Simpson et al. [3]; Zhang [4]; Paizis et al. [5]; Simpson et al. [6]).

4 Conclusion

In this paper we presented the numerical results on the cosmic-ray modulation in the Fisk-type HMF obtained by the calculation based on the SDE method. The sample trajectories of protons in the Fisk-type HMF shows clear tendencies to deviate from the typical drift pattern in the Parker HMF. Simulated spectra for the galactic cosmic-ray protons and antiprotons agrees well with BESS results in 1997 assuming the Fisk-type HMF. The resultant latitudinal dependence of the proton intensities in the Fisk-type HMF may explain the observations by Ulysses.

References

[1] E. N. Parker, Astrophys. J., 1958, **128**: 664-676
[2] L. A. Fisk, J. Geophys. Res., 1996, **101**(A7): 15,547-15,553
[3] J. A. Simpson, J. J. Connell, C. Lopate, R. B. McKibben, and M. Zhang, Geophys. Res. Lett., 1995, **22**(23): 3337-3340
[4] M. Zhang, Astrophys. J., 1997, **488**: 841-853
[5] C. Paizis et. al., J. Geophys. Res., 1999, **104**(A12): 28,241-28,247
[6] J. A. Simpson, M. Zhang, and S. Bame, Astrophys. J., 1996, **465**: L69-L72
[7] S. Miyake and S. Yanagita, In Proc. 29th Int. Cosmic-ray Conf. (Pune), 2005, **2**, 203-206
[8] Y. Yamada, S. Yanagita, and T. Yoshida, Geophys. Res. Lett., 1998, **25**(13): 2353-2356
[9] M. Zhang, Astrophys. J., 1999, **513**: 409-420
[10] R. A. Burger, H. Moraal, and M. S. Potgieter, In Proc. 20th Int. Cosmic-ray Conf. (Moscow), 1987, **3**: 283-286
[11] R. A. Burger and M. Hitge, Astrophys. J., 2004, **617**: L73-L76
[12] L. A. Fisk, T. H. Zurbuchen, and N. A. Schwadron, Astrophys J., 1999, **521**: 868-877
[13] J. Schou et al., Astrophys. J., 1998, **505**: 390-417
[14] J. Giacalone, Adv. Space Res., 1999, **23**(3): 581-590
[15] J. Giacalone, J. Geophys. Res., 2001, **106**(A8): 15,881-15,887
[16] Y. Shikaze et al., Astropart. Phys., 2007, **28**: 154-167
[17] I. V. Moskalenko, A. W. Strong, J. F. Ormes, and M. S. Potgieter, Astrophys. J., 2002, **565**: 280-296
[18] S. Orito et al, Phys. Rev. Lett., 2000, **84**: 1070-1081